Stereoselectivity and Chiral Recognition in Copper(I) Olefin Complexes with a Chiral Diamine

Luigi Cavallo, Maria E. Cucciolito, Alberto De Martino, Federico Giordano, Ida Orabona, and Aldo Vitagliano*[a]

Dedicated to Prof. Fausto Calderazzo on the occasion of his 70th birthday

Abstract: Trigonal copper(I) complexes of the chiral bidentate ligand (1*S*,2*S*)-*N*,*N*′-Bis-(mesitylmethyl)-1,2-diphenyl-1,2-ethanediamine ((*S*,*S*)-**1**) have been prepared with hydrocarbon olefins, as well as with allylic alcohols and ethers. The stereochemistry of the complexes has been investigated by ^{1}H NMR spectroscopy and by combined quantum mechanics and molecular mechanics (QM/MM) computational methods. The coordinated chiral nitrogen atoms can display equal (*R*, *R*) or opposite (*R*, *S*) configuration, the latter being disfavored if steric hindrance is present above and below the coordination plane. Although the complexes exist as rapidly equilibrated mixtures of stereoisomers, one of these is often dominant, and prochiral olefins are coordinated with high enantioface selection. In addition, the [(*S*,*S*)-**1**]-Cu$^+$ fragment selectively recognizes the R enantiomer of secondary allylic alcohols and ethers, as confirmed by the X-ray crystal structure analysis of the adduct with (*R*)-1-buten-3-ol. The reasons for the observed selectivities have been elucidated, and lead to some implications which are consistent with the enantioselection observed in catalytic cyclopropanation reactions promoted by copper complexes of the same ligand.

Keywords: chiral diamine · chirality · copper · enantioselectivity · olefin

Introduction

Chiral recognition in the coordination of olefins to chiral transition metal fragments is a topic of interest,[1] especially because of its involvement in metal-promoted enantioselective syntheses.[2] Although binding selectivity is often not the controlling factor in metal-catalyzed asymmetric reactions,[3] it is more likely to be so in stoichiometric processes. Whether or not enantioselectivity at the stage of π-complex formation determines the final outcome of an asymmetric transformation, its assessment remains essential for developing an understanding of the whole process. Moreover, since the induction of asymmetry is usually dominated by steric effects, observable ground state π complexes can be reliable steric models for intermediates or transition states having similar geometry, even if different metals or reactions are involved.[4]

Two different aspects of chiral recognition that can be considered are enantioface selectivity in the coordination of a prochiral olefin (which becomes diastereoface selectivity in the case of a chiral olefin) and enantiomer selectivity in the coordination of a racemic chiral olefin. The latter is relevant to the thermodynamic[5] or kinetic[6] resolution of racemic olefins. These subjects have been investigated for a variety of transition metal chiral moieties,[1] but only very recently has stereoselectivity in copper(I) olefin complexes attracted interest[7] in connection to asymmetric catalytic cyclopropanation/aziridination[7,8] and allylic substitution[9] reactions. The diamine *N*,*N*′-bis-(mesitylmethyl)-1,2-diphenyl-1,2-ethanediamine (**1**) was originally prepared by Corey et. al.[10] and used as a very effective controller ligand for the enantioselective[10] and diastereoselective[11] dihydroxylation of olefins by osmium tetroxide. More recently, its use in copper chemistry has been reported by Kanemasa et. al. (asymmetric catalytic cyclopropanation of styrenes[12]) and by some of us (stoichiometric resolution of secondary allylic alcohols via Cu^I complexes).[5a] We have also reported the isolation of trigonal-bipyramidal Pt^{II} olefin complexes of **1**, in which relevant stereoselectivity effects were observed.[13] Our previous results[5a,13] prompted us to a deeper investigation of the Cu^I olefin complexes of **1**. Our aim was both to investigate the stereochemistry of diamine and olefin coordination in a purely trigonal environment (i.e. in the absence of the constraints added by the axial ligands), and to rationalize

[a] Prof. Dr. A. Vitagliano, Dr. L. Cavallo, Dr. M. E. Cucciolito, Dr. A. De Martino, Prof. Dr. F. Giordano, Dr. I. Orabona
Dipartimento di Chimica
Università di Napoli "Federico II"
Via Mezzocannone 4, 80134 Napoli (Italy)
Fax: (+39) 0815527771
E-mail: alvitagl@unina.it

  0947-6539/00/0607-1127 $ 17.50+.50/0

the remarkable chiral recognition observed in the formation of the Cu^{I} complexes with allylic alcohols.[5a] Here we report our results, which include combined quantum mechanics and molecular mechanics (QM/MM) studies of selected species and the X-ray crystal structure analysis of the complex with the representative allylic alcohol (*R*)-1-buten-3-ol.

Results and Discussion

Synthesis of the complexes: A convenient starting material for the preparation of the olefin adducts is the complex $[Cu(MeCN)_4]X$ ($X = BF_4$ or ClO_4). By treating it with the stoichiometric amount of the diamine (*S*,*S*)-**1**[14] and an excess of the appropriate olefin (5 equivalents if not gaseous) under an oxygen-free atmosphere, the ternary complexes **2**–**10** are formed in a fast equilibrium reaction (Scheme 1). This

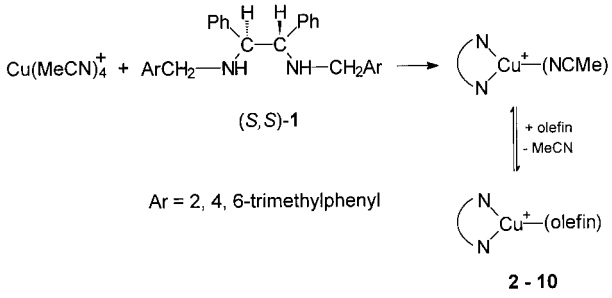

2 olefin = ethylene
3 olefin = propene
4 olefin = 1-pentene
5 olefin = *E*-2-butene
6 olefin = *Z*-2-butene
7 olefin = 1-propen-3-ol
8 olefin = 1-buten-3-ol
9 olefin = 1-octen-3-ol
10 olefin = 3-methoxy-1-butene

Scheme 1.

reaction is quite general, and in most cases the products could be crystallized directly from the reaction mixture as colorless needles. The rapid reversibility of the olefin coordination was nicely indicated by the sudden redissolution of the crystals, which occurred in the case of gaseous olefins (ethylene and propene) upon our first attempts to improve the yield by concentrating the solution in vacuo. Indeed, ^{1}H and ^{13}C NMR spectra of the complexes indicated that the rate of olefin exchange and nitrogen inversion is quite high (especially in the presence of coordinating impurities), resulting in broad signals for most of the protons or carbons of the complex at room temperature. Accordingly, to obtain spectra suitable for a proper characterization of the species, low temperature measurements were necessary in all cases.

Dynamic stereochemistry of the complexes, general considerations: The diamine (*S*,*S*)-**1** contains, besides the two chiral carbon centers, two chiral nitrogen centers, which quickly invert in the free ligand but whose chirality is "frozen" upon coordination. As a consequence different diastereomers can in principle be formed, depending on the configuration adopted by the coordinated nitrogen centers. The number of possible diastereomers can further increase depending on the symmetry of the coordinated olefin. In the case of the most symmetric ethylene ligand three isomers are possible, differing only in the configuration of the nitrogen atoms. In the extreme case of an asymmetrically substituted chiral olefin up to 16 isomers could be formed, depending on the configuration of the nitrogen atoms, on which enantiomer is coordinated, and on which diastereoface is coordinated. However, the ability to detect and identify by NMR spectroscopy the actual isomers at equilibrium and to measure their relative amounts (thus getting the desired information about stereoselection in the assembly of the complex) is bound to the rates of the various dynamic processes taking place in solution and interconverting the isomers. Six different dynamic processes can take place in solution, five of which have been experimentally revealed and four of which can result in isomer interconversion: a) exchange of the N–N ligand; b) nitrogen inversion; c) olefin exchange; d) olefin rotation; e) rotation around the C–Ph bonds in the diamine backbone; f) rotation around the C–mesityl bonds in the diamine "arms". A general qualitative discussion of the occurrence of these processes for complexes **2**–**10** seems worthwhile.

a) N–N Ligand exchange: This process would interconvert all of the isomers that differ in the configuration of the coordinated nitrogen atoms. It is actually the slowest one and did not affect the NMR measurements, since well-separated signals were observed for the protons of the coordinated diamine and those of added free diamine for all of the complexes up to 300 K. It is also worth noting that the addition of one equivalent of free diamine to the NMR samples did not displace the olefin.

b) Nitrogen inversion: For the nitrogen atoms the most stable configuration is expected to be the one opposite to that of the chiral carbon atoms, so that the bulky substituents of the five-membered chelate ring can lie in a *trans*-equatorial arrangement. The four ligand atoms involved in the chelate ring should thus be arranged as *R*, *S*, *S*, *R*, as found in bipyramidal Pt^{II} complexes.[13] However, the NMR spectra revealed the presence of isomers with inverted configuration of one nitrogen atom, namely *R*, *S*, *S*, *S*. With two exceptions, these isomers were generally observed as minor species (Table 1) and their abundance was significantly decreased when the temperature was lowered. At 300 K, the interconversion between these isomers caused broadening of the NMR signals of the diamine ligand in most complexes, allowing the qualitative estimation of nitrogen inversion as the second slowest dynamic process taking place in solution. In the absence of coordinating impurities, the nitrogen inversion was frozen on the NMR time scale in the range 280–290 K.

c) Olefin exchange: This process causes interconversion of isomers which differ in terms of the enantioface (or diastereoface) that is coordinated or in terms of the enantiomeric olefin that is coordinated (in the case of racemic chiral alkenes). As expected for coordinatively unsaturated species in which bimolecular ligand exchange processes are favored, the rate of olefin exchange was found to be substantially increased by the

0947-6539/00/0607-1128 $ 17.50+.50/0 *Chem. Eur. J.* **2000**, *6*, No. 7

Table 1. Diastereomeric distribution of [Cu((*S*,*S*)-**1**)(olefin)]$^+$ complexes.[a]

Complex	Olefin	% at 243 K	*N*,*N* configuration	Coordinated enantioface[b]
2a	ethylene	70	*R*, *R*	–
2b	ethylene	30	*R*, *S*	–
3a	propene	86	*R*, *R*	*re*
3b	propene	8	*R*, *S*	*re*
3c	propene	6	*R*, *S*	*si*
4a	1-pentene	83	*R*, *R*	*si*
4b	1-pentene	10	*R*, *S*	*si*
4c	1-pentene	7	*R*, *S*	*re*
5a	*E*-2-butene	>97	*R*, *R*	*re*
6b	*Z*-2-butene	≈ 75[c]	*R*, *S*	–
7a	allyl alcohol	>95	*R*, *R*	*si*
8a[d]	1-buten-3-ol	>95	*R*, *R*	*si*[e]
9a[d]	1-octen-3-ol	94	*R*, *R*	*si*
10a[d]	3-methoxy-1-butene	95	*R*, *R*	*si*

[a] Equilibrium populations in CD_2Cl_2/CD_3OD 9/1. [b] Configuration assigned on the basis of MM calculations and ^{1}H NMR data. See ref. [20] about *re-si* conventions. [c] $T = 273$ K. [d] Data for the isolated diastereomer containing the *R* olefin. [e] Unequivocally assigned from the X-ray structure analysis.

presence of free olefin. In addition, it was found to be much faster (see next section) for the C_2-symmetrical species (*R*, *S*, *S*, *R*) than for the asymmetric species (*R*, *S*, *S*, *S*). In the absence of coordinating impurities and below 243 K, the olefin exchange process was generally frozen on the NMR time scale for all of the complexes investigated.

d) Olefin rotation: Different rotamers can, in principle, exist and be interconverted by this process only if both the coordinated diamine and the coordinated olefin lack a C_2 axis. They would therefore be detected only in the case of the *R*, *S*, *S*, *S* species. However, olefin rotation can be revealed if one of the two fragments lacks a C_2 axis. If the diamine backbone is C_2 symmetrical but the olefin is not, hindered rotation can be revealed by removal of the equivalence of the two halves of the diamine ligand. Conversely, if the olefin is symmetrical (ethylene or *E*-2-butene) but the diamine backbone is not C_2-symmetrical (*R*, *S*, *S*, *S* species), hindered rotation can be revealed by removal of the equivalence of mutually *trans* olefinic substituents. The rate of olefin rotation was found to be substantially lower for the allylic alcohol complexes than for complexes of hydrocarbon olefins. In both the propene and 1-pentene complexes **3** and **4** free rotation was observed down to 200 K, while in the propenol and butenol complexes it was frozen in the temperature range 210–220 K.

e), f) Rotation around the C–Ph and C–mesityl bonds: Hindered rotation of the phenyl rings was revealed for all complexes at temperatures below 270 K by the nonequivalence of the *ortho* and *meta* protons within each phenyl group. Freezing of the rotation of the mesityl rings was revealed in the temperature range 210–220 K by the nonequivalence of the *ortho* methyl groups within each mesityl group. These processes were also detected in the same temperature ranges for the bipyramidal platinum species.[13] They are not particularly relevant to the stereochemistry of the complexes, since they are not connected with isomer interconversion. Nevertheless they provide evidence of the steric constraints imposed on the diamine ligand by coordination, resulting in an overall rigidity, which is consistent with the high stereoselection observed in these species (as discussed below).

Dynamic stereochemistry of the complexes, specific aspects: In this section we shall discuss the stereochemistry of representative complexes, as inferred from ^{1}H NMR data. The isomers that were observed in solution, their relative abundances, and configurational assignments are reported in Table 1 . Relevant ^{1}H NMR data are given in Table 2.

*Complex **2**:* The ethylene complex **2** exists in solution as an equilibrium mixture of two isomers **2a** and **2b**. Figure 1 shows the ^{1}H NMR spectra of **2** (400 MHz), recorded at 283 K in CD_2Cl_2 (A) and at 223 K in CD_2Cl_2/CD_3OD 9/1 (B), together with the assignments of the various signals. Although in this case stereoselection in the olefin coordination is not a concern, we will discuss these spectra in detail, because they are illustrative of a number of features, which are common to the other complexes. The presence of two different species is apparent from both spectra. For one species (**2a**) protons belonging to different sides of the diamine ligand appear to be equivalent, while for the other species (**2b**) protons belonging to different sides of the diamine ligand give different sets of signals. Therefore the C_2-symmetric configuration of the diamine skeleton (*R*, *S*, *S*, *R*) can be assigned to **2a**[15] and the asymmetric configuration (*R*, *S*, *S*, *S*) can be assigned to **2b**. Particularly relevant is the difference in the chemical shifts of H^4 and $H^{4'}$ of the diamine backbone in **2b**. In spectrum A the apparent triplet due to H^4 at $\delta = 4.53$ is almost overlapped by the corresponding apparent doublet of doublets ($\delta = 4.49$) from the symmetrical species **2a**, while the doublet of doublets due to $H^{4'}$ appears 1 ppm downfield ($\delta = 5.49$). The latter can confidently be assigned to the proton vicinal to the N atom having inverted *S* configuration, not only because of the large downfield shift,[17] but also because its coupling to the vicinal NH proton is much smaller than for H^4 (5.4 Hz versus 12.4 Hz), consistent with an equatorial–axial arrangement for the CH–NH protons. This feature can be used as a diagnostic tool to assign (or to exclude) an asymmetric configuration (*S*, *S*, *S*, *R*) to the diamine backbone in cases in which the lack of C_2 symmetry can be attributed to some other reason (e.g. hindered rotation of an asymmetric olefin).

The detection of such a high relative concentration of the asymmetric species **2b** (at 283 K in CD_2Cl_2 **2b** is the major isomer) was actually surprising, because in the case of trigonal bipyramidal Pt^{II} complexes[13] only the symmetric isomer was observed. However, while molecular mechanics studies made on osmium complexes[16] did not mention such asymmetric species, a QM/MM analysis of **2** in this work calculated **2b** to be only 2 kJ mol^{-1} above **2a**. Most likely, the asymmetric species **2b** is not much less favored than **2a** because of the lack of the steric constraints, which in the above-cited bipyramidal and octahedral species are imposed by the axial ligands. It is worth noting that from the isomeric populations determined in CD_2Cl_2/CD_3OD (9/1) at various temperatures in the range 230–300 K, **2b** was actually found to be enthalpically

Table 2. Selected ^{1}H NMR data for [Cu(*S*,*S*-**1**)(olefin)]ClO_4 complexes.[a]

	Diamine protons						Olefinic protons			Others
Complex	H^2	$H^{2'}$	H^3	$H^{3'}$	H^4	$H^{4'}$	H^Z	H^E	H^5	
2a[b]	3.85 (2H, d)		3.48 (2H, d)		4.43 (2H)		3.14 (2H, br); 2.96 (2H, br)			
2b[b]	3.82 (d)	3.66 (d)	3.62 (d)	3.17 (d)	4.57 (br)	5.24 (br)	2.72 (2H, br); 3.24(2H, br)			
3a[c]	3.92 (2H, d)		3.55 (2H, d)		4.45 (2H)		3.21 (br)	3.01 (br)	4.22 (br)	0.70 (3H, br, =CH*Me*)
3b	3.91 (d)	3.71 (d)	3.77 (d)	3.22 (d)	4.53 (d)	5.32 (d)	2.47 (d)	3.45 (d)	4.11 (br)	0.61 (3H, d, =CH*Me*)
3c	3.82 (d)	3.71 (d)	3.61 (d)	3.22 (d)	4.56 (d)	5.29 (d)	2.87 (2H, m)		3.25 (m)	1.08 (3H, d, =CH*Me*)
4a[d]	3.95 (2H, d)		3.54 (2H, d)		4.50 (2H)		2.88 (d)	3.20 (br)	4.17 (br)	0.45 (1H, br, =CHC*H*H) 1.07 (1H, br, =CHCH*H*)
4b	3.91 (d)	3.77 (d)	3.70 (d)	3.20 (d)	4.52 (d)	5.32 (d)	2.43 (d)	3.41 (d)	4.04 (m)	0.19 (1H, br, =CHC*H*H), 1.22 (1H, br, =CHCH*H*)
4c	3.83 (d)	3.63 (d)	3.70 (d)	3.20 (d)	4.55 (d)	5.32 (d)	2.86 (d)	2.89 (d)	3.30 (br)	1.12 (1H, br, =CHC*H*H) 1.48 (1H, br, =CHCH*H*)
5a[e]	4.02 (2H, d)		3.49 (2H, d)		4.60 (2H)		3.75 (2H, br)			0.66 (6H, br, =CH*Me*)
6b[f]	3.82 (d)	3.66 (d)	3.71 (d)	3.20 (d)	4.40 (d)	5.40 (d)	3.96 (1H, m); 3.30 (1H, m)			1.00 (3H, d, =CH*Me*) 0.59 (3H, d, =CH*Me*)
7a[b]	3.88 (2H, d)		3.49 (2H, d)		4.38 (2H, br)		3.07 (br)	3.20 (br)	4.17 (br)	3.07 (1H, br, =CHC*H*H)
8a[d]	3.82 (2H, br)		3.47 (2H, d)		4.31 (2H, br)		2.94 (d)	3.23 (d)	4.12 (dd)	0.68 (3H, d, CH(OH)*Me*)
8c′	3.82	3.77 (d)	3.60(d)	3.16(d)	4.50 (d)	5.10 (d)	2.81 (d)	3.09 (d)	3.29 (dd)	
9a[d]	3.84 (2H, br)		3.46 (2H, d)		4.33 (2H, br)		2.98 (d)	3.21 (d)	4.12 (m)	
10a[d]	3.84 (2H, br)		3.49 (2H, d)		4.35 (2H, br)		3.04 (d)	2.99 (d)	4.17 (m)	0.66 (3H, d, CH*Me*) 3.08 (3H, O*Me*)

[a] Ar = 2,4,6-trimethylphenyl. Spectra were recorded in CD_2Cl_2/CD_3OD 450 μL/50 μL. The following abbreviations were used for describing NMR multiplicities: no attribute, singlet; d, doublet; dd, double doublet; m, multiplet; br, broad. [b] Spectrum recorded at T = 243 K. [c] Spectrum recorded at T = 258 K. [d] Spectrum recorded at T = 253 K. [e] Spectrum recorded at T = 233 K. [f] Spectrum recorded at T = 273 K.

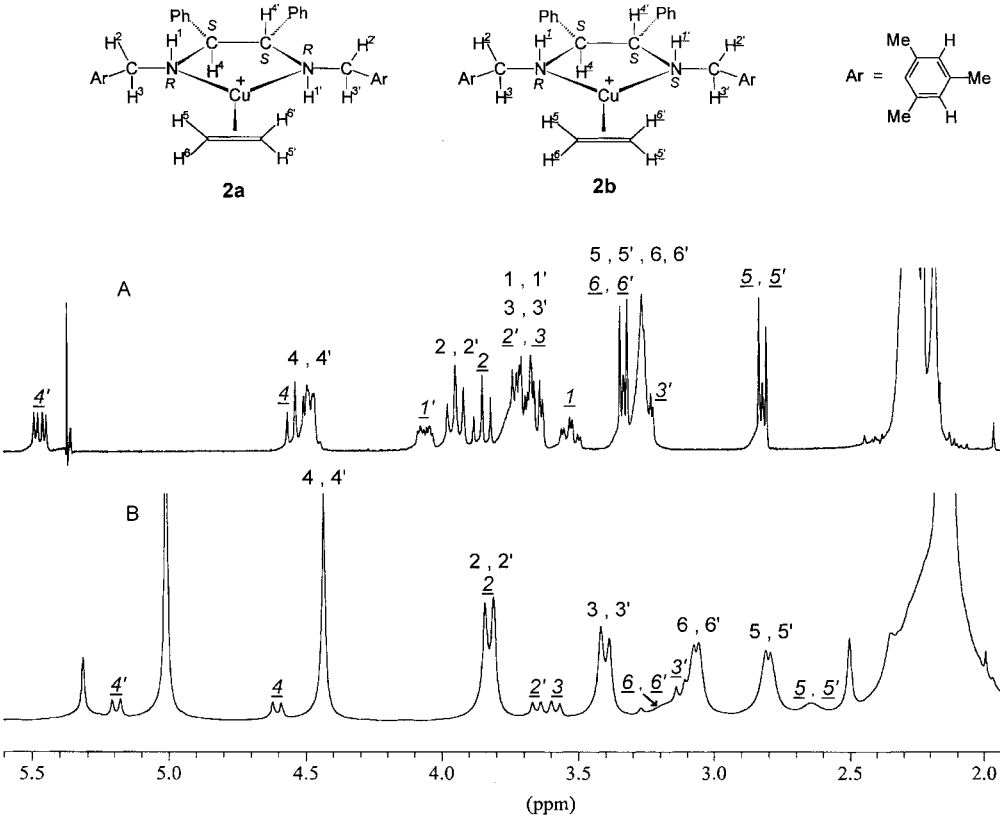

Figure 1. Selected portion of the 400 MHz ^{1}H NMR spectrum of **2** (**2a** + **2b**): A) CD_2Cl_2, 283 K; B) CD_2Cl_2/CD_3OD 10/1, 223 K. Underlined assignments refer to **2b**.

disfavored over **2a** by about 6 kJ mol^{-1} but entropically favored by nearly 20 J mol^{-1} K^{-1}.

Another relevant point illustrated by the spectrum run at 283 K (A) is the relative inertness to olefin exchange in **2b** compared with **2a**. While the ethylene protons of **2a** give rise to a broad singlet at $\delta = 3.25$, those of **2b** appear as a sharp AA′XX′ multiplet ($\delta_{AA'} = 3.33$ and $\delta_{XX'} = 2.82$). At 223 K (spectrum B), the ethylene protons of **2a** appear as an

0947-6539/00/0607-1130 $ 17.50+.50/0 *Chem. Eur. J.* **2000**, *6*, No. 7

AA′XX′ multiplet ($\delta_{AA'} = 3.06$ and $\delta_{XX'} = 2.81$), while those of **2b** give two broad signals ($\delta_{AA'} = 3.20$ and $\delta_{XX'} = 2.65$). In the presence of an equimolar amount of free olefin, the coalescence temperatures of the ethylene protons for the two isomers are 250 K for **2a** and 315 K for **2b**. Even taking into account that the exchange rate at coalescence would be about twice as large for **2b** as for **2a**, because of the larger chemical shift difference between the geminal ethylene protons, we can estimate the exchange rate in **2b** to be a couple of orders of magnitude (if not more) slower than in **2a**. In spectrum B the ethylene proton pattern of **2b** indicates that olefin rotation around the Cu–double bond axis is still moderately fast on the NMR time scale. On further cooling (203 K), the signals coalesce, disappearing into the baseline as a consequence of slower rotation at this temperature.

A final feature worth pointing out is the unusually high field at which the ethylene proton resonances appear (see above), compared with the range $\delta = 4.8-4.0$ commonly found in Cu^+ complexes.[18] Moreover, the resonances move further upfield when the temperature is lowered (compare spectra A and B in Figure 1). This high-field shift is strong evidence that the protons (especially H^5 and $H^{5'}$) are located in the shielding cone of the mesityl rings, thereby indicating that in the most stable conformation the mesityl rings protrude forward to envelop the sides of the third coordinative position. When the temperature is lowered, the population of the most stable conformation increases, and accordingly, the average shielding effect on the olefinic protons proximal to the mesityl rings increases.[19]

Complex 3: The dynamics of this complex closely resembles that of the ethylene complex **2**, and the discussion will be focused on the stereochemistry of the species. Six diastereomers are in principle possible for the propene complex under the condition of fast rotation around the Cu–olefin bond. As revealed by the ^1H NMR spectra, the complex exists in solution as an equilibrium mixture of three detectable isomers (Tables 1 and 2, Figure 2). The spectrum of the major isomer (**3a**) shows equivalence between the two halves of the diamine ligand, indicating a C_2-symmetric structure (averaged by fast rotation around the Cu–olefin bond). The *R*, *S*, *S*, *R* configuration can consequently be assigned to the diamine backbone.[15] As for the propene binding, the QM/MM calculations indicate that coordination of the *re*[20] enantioface (structure **3a** in Figures 2 and 3) is favored by 5 kJ mol^{-1} relative to the coordination of the *si* enantioface (Figure 3C), thereby allowing assignment of structure **3a** to the major isomer. The calculated optimal conformation of **3a** is actually shown to be predominant in solution by the high field at which the propene methyl resonance of **3a** appears ($\delta = 0.70$ at 258 K), which indicates that the methyl group lies in the shielding cone of the adjacent mesityl ring (Figure 2) and thereby supports the assignment of the *re* configuration to the coordinated enantioface. The second and third isomers (**3b** and **3c**, respectively) both show inequivalent halves of the diamine ligand, with the signal of one of the two PhCH protons appearing at $\delta \approx 5.3$ and the other at $\delta \approx 4.5$. This unambiguously indicates that in both **3b** and **3c** the configuration of one nitrogen atom is inverted compared with that in

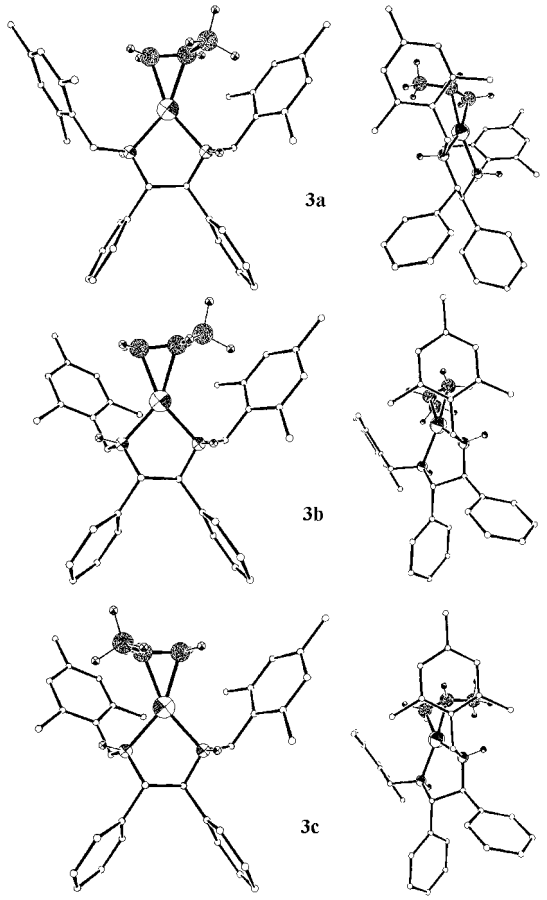

Figure 2. Three lowest energy QM/MM-optimized geometries of the propene complex **3**, corresponding to the stereoisomers **3a**, **3b**, and **3c**, seen along the normal to the N-Cu-N plane (left) and along the normal to one mesityl ring (right), showing the olefinic proton(s) located in the shielded region.

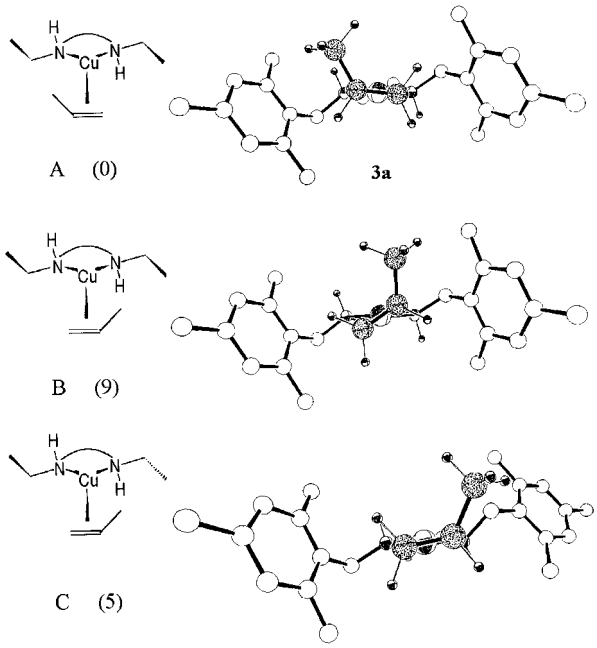

Figure 3. QM/MM-optimized geometries for propene coordination to the fragment with *R*, *S*, *S*, *R* configuration, with their relative energies (kJ mol^{-1}) given in parentheses (the phenyl groups in the back have been omitted): A) C_2-symmetric diamine conformation, *re* face coordinated (**3a**); B) and C) *si* face coordinated.

3a, resulting in an *R*, *S*, *S*, *S* backbone configuration for the diamine ligand. To establish the difference between **3b** and **3c**, we can consider that the two possible configurations *R*, *S*, *S*, *S* and *S*, *S*, *S*, *R* would be interconverted by a 180° rotation of the olefin molecule. Therefore they are indistinguishable under the condition of free rotation of the olefin, which is the case (as shown above) at temperatures above 213 K. This takes us to the conclusion that **3b** and **3c** must differ from each other by the olefinic enantioface that is coordinated and not by which nitrogen atom is inverted. It is possible to go even further, trying to establish which enantioface is coordinated in each isomer. Here we consider that in **3b** the signals of both the methyl and methine protons of the propene ligand appear very close to the corresponding ones in the major isomer **3a** (see Table 2). In contrast, the signals of the methylene protons are very much displaced, and in opposite directions, from the corresponding ones in **3a**. This indicates that in going from **3a** to **3b** the steric environment on the side of the MeCH= moiety is kept almost unchanged, while the steric environment on the side of the $=CH_2$ moiety undergoes a substantial change. It is therefore very likely that the only difference between **3a** and **3b** is the configuration of the nitrogen atom on the side of the $=CH_2$ propene moiety, the coordinated olefinic enantioface being the same (*re*). It is worth noting that the large upfield shift of the H^Z proton ($\delta =$ 2.47 in **3b** versus $\delta = 3.21$ in **3a**) is in contrast to the downfield shift of the H^E proton ($\delta = 3.45$ in **3b** versus $\delta = 3.01$ in **3a**). This suggests that in the predominant conformation of the molecule the H^Z proton is situated on the side of the nitrogen atom having inverted *S* configuration, just in the middle of the shielding cone of the mesityl ring, which thus lies below the coordination plane facing the H^Z proton. This is nicely confirmed by the QM/MM optimized geometries reported in Figure 2. In the last isomer **3c**, the opposite enantioface (*si*) must be coordinated. Comparing the propene chemical shifts of **3c** with those of **3a**, the largest differences are now found for the methyl protons which move downfield ($\delta = 1.08$ in **3c** versus $\delta = 0.70$ in **3a**) and especially for the methine H^5 proton which moves upfield ($\delta = 3.25$ in **3c** versus $\delta = 4.22$ in **3a**). This suggests that in the predominant conformation of **3c**, the diamine skeleton is arranged in the same way as in **3b**, but the propene molecule is flipped from left to right, so as to bring the H^5 proton in the shielding cone of the mesityl ring lying below the coordination plane. This is also in agreement with the results of QM/MM modeling (see Figure 2).

*Complex **4**:* The stereochemistry of the 1-pentene complex closely resembles that of the propene complexes discussed above, indicating that substitution of a flexible chain for the methyl group does not alter the overall steric requirements of the complex. The diastereomeric populations are given Table 1 and relevant ^{1}H NMR data are listed in Table 2.

*Complex **5**:* Six diastereomers are possible for the *E*-2-butene complex. Based on the results obtained for the propene complex **3** and on the configurational assignments made to the three isomers **3a**, **3b**, and **3c**, the presence of only one largely predominant species for **5** would be expected. This because in each of the favored conformations of complexes **3b** and **3c** (Figure 2), the substitution of a methyl group for the H^Z proton would presumably produce a severe steric interaction with a mesityl ring. Indeed, the only isomer which could be identified in solution revealed the C_2-symmetric structure **5a** and its abundance was estimated to be larger than 97% at 243 K.

*Complex **6**:* For the *Z*-2-butene complex there is no concern about enantioface selection. Nevertheless this complex was prepared and investigated to give independent support to the whole picture of the mutual influence between the geometry of olefin coordination and the configuration adopted by the nitrogen atoms. The same kind of arguments as for complex **5** (but with opposite conclusions) suggest a substantial destabilization of the *R*, *S*, *S*, *R* arrangement of the diamine backbone for **6** (see Figure 3A, imagining the addition of a *Z*-methyl group to the propene ligand). To confirm these expectations, the major isomer present in solution (**6b**, ≈75% abundance at 273 K) did indeed reveal an asymmetric *R*, *S*, *S*, *S* configuration of the diamine moiety.

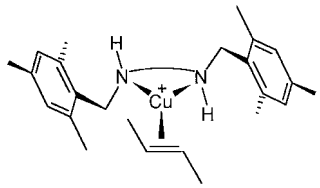

5b

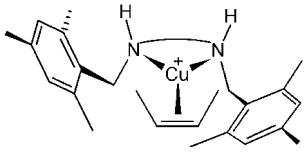

6b

*Complex **7**:* From a steric point of view, there should be little difference between the propene complex **3** and the allyl alcohol complex **7**. Also, the electronegative OH substituent is not expected to have much of an effect on the intrinsic strength of the copper–olefin bond, which is known to be minimally influenced by the electronic effects of the substituents.[18e] In spite of this, significant differences were found in both the diastereomeric distribution and the dynamic behavior of complex **7**, compared with **3**. Although species with inverted configuration of one nitrogen atom (*R*, *S*, *S*, *S* backbone) could be detected in solution, their abundance was substantially lower than for the corresponding species (**3b** and **3c**) of the propene complex (Table 1). The rate of olefin exchange for the major isomer **7a** was found to be lower than for **3a**. Thus, in the presence of an equimolar excess of free allyl alcohol, the exchange was frozen on the NMR time scale at 253 K, while in the case of **3a** the corresponding temperature was 20 K lower. Also, rotation of the olefin around the metal–double bond axis was frozen at about 223 K, while no evidence of hindered rotation was detected down to 200 K in the case of **3a**. To test the relative stabilities of **3a** and **7a**, an

0947-6539/00/0607-1132 $ 17.50+.50/0 *Chem. Eur. J.* **2000**, *6*, No. 7

equimolar amount of allyl alcohol was added to an NMR sample of **3a** and the equilibrium abundances of **3a** and **7a** were measured at 233 K. The equilibrium constant for the exchange reaction could thus be estimated to be $K = 5$. All these data indicate the allyl alcohol complex **7a** to be both kinetically less labile and thermodynamically more stable than the propene complex **3a**, a result that is consistent with previous findings, which suggest an oxygen–copper interaction in Cu^+ adducts of allylic alcohols.[21]

Complex **8**: Although 12 diastereomers are in principle possible for this complex if the racemic olefin 1-buten-3-ol is used in the synthesis (16 in the case of hindered rotation around the Cu–olefin bond), one largely dominant species (**8a**, > 95% abundance) was detected in solution by ^{1}H NMR spectroscopy. This indicates both a large preference for the coordination of one diastereoface of the olefin (*si*,[20] as suggested by the above result) and a large selectivity for the coordination of one enantiomer. The selected enantiomer has the *R* configuration, as proved independently by X-ray diffraction analysis (Figure 4) and by decompostion of the

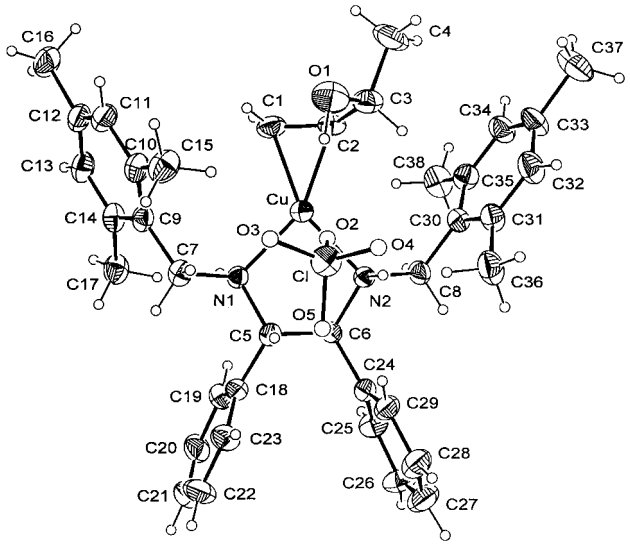

Figure 4. ORTEP view of [Cu((*S*,*S*)-**1**)((*R*)-1-buten-3-ol)]ClO_4 (**8a**).

complex and recovery of the optically active allylic alcohol.[5a] It was important to establish to what extent the almost exclusive formation of the complex with the (*R*)-alcohol was due to the selective coordination of one enantiomer rather than to a selective crystallization of one diastereomeric adduct. To this purpose, we isolated the allylic alcohol of the opposite chirality (i.e. (*S*)-1-buten-3-ol) through its Cu^I complex with (*R,R*)-**1**, and added an excess of it to an NMR sample of **8a**. Small signals appeared in the spectrum which could unambiguously be assigned to the diastereomeric complex **8c′** (see Table 2), containing (*S*)-1-buten-3-ol (Figure 5C). The same signals were almost undetectable when an excess of racemic butenol was added to the complex. From the ^{1}H chemical shifts of complex **8c′** (see Table 2) and the previous discussion on the propene complexes **3** it is possible to infer that **8c′** has a structure in which the diamine backbone has an *R*, *S*, *S*, *S* configuration and the *re* diastereoface is

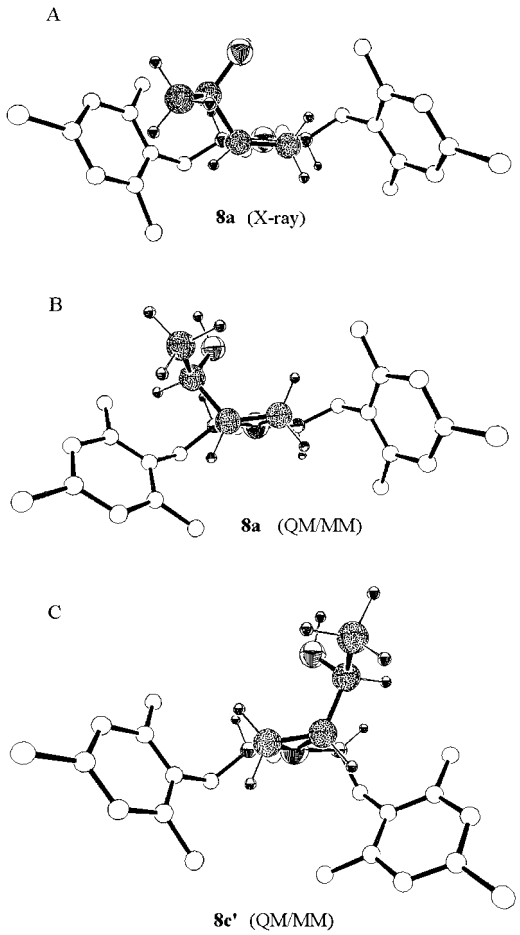

Figure 5. Experimental and calculated structures of **8**. A) X-ray structure of **8a**; B) QM/MM-optimized geometry of **8a**; C) QM/MM-optimized geometry of the complex with (*S*)-1-buten-3-ol (**8c′**).

coordinated (Figure 5C). The above findings definitely prove that chiral recognition of the (*R*)-1-buten-3-ol by the [(*S*,*S*)-**1**-Cu]$^+$ fragment takes place in solution and therefore crystallization plays a minor role, if any, in the resolution. By knowing the analytical composition of the mixture and by integration of the appropriate NMR signals, the equilibrium constant for the exchange of the two enantiomers on the [(*S*,*S*)-**1**-Cu]$^+$ fragment could be estimated to be $K \approx 40$.

Molecular structure of ((*S*,*S*)-1)((*R*)-1-buten-3-ol)copper(I) perchlorate (8a): The molecular structure of the complex, together with the atom-labeling scheme are shown in Figure 4. The Cu^I ion is coordinated to the two N atoms of the diamine and to the olefinic double bond of the allylic alcohol in the expected trigonal-planar geometry. The dihedral angle between the planes defined by Cu, N1, and N2 and by Cu, C1, and C2 is 5(1)°, while copper and the four-coordinate atoms are coplanar within 0.05(1) Å. The diamine ligand exhibits an approximate C_2 symmetry and the two chiral nitrogen atoms display the same configuration, opposite to that of the chiral carbon atoms, resulting in the overall *R*, *S*, *S*, *R* configuration of the backbone of the chelate ring. The olefin ligand is present as the *R* enantiomer and the *si*-enantioface[20] of the double bond is coordinated, keeping the olefin substituent and the nitrogen side chain in an *anti* orientation to each

other. Each perchlorate anion lies nearly halfway between two cations and is linked to one of them by a weak bifurcated hydrogen bond, bridging O2 to both N2 (O–N 3.11(1) Å) and O1 (O–O 3.06(1) Å).

Selected bond lengths and angles are presented in Table 3. The Cu–N bond lengths, 2.055(5) and 2.032(5) Å, fall in the middle of the range (1.93–2.16 Å) observed in similar

Table 3. Selected bond lengths [Å] and valence angles [°] with their esds in parentheses for **8a**.

Cu–N1	2.055(5)	O1–C3	1.40(1)
Cu–N2	2.032(5)	C1–C2	1.36(1)
Cu–C1	2.011(9)	C2–C3	1.54(1)
Cu–C2	2.036(8)	C3–C4	1.53(1)
N1-Cu-N2	87.7(2)	Cu-C1-C2	71.3(5)
C1-Cu-C2	39.3(3)	Cu-C2-C1	69.4(5)
Cu-N1-C5	105.8(4)	C1-C2-C3	124.0(8)
Cu-N2-C6	105.5(4)		

complexes.[22] Likewise, the two Cu–C(olefin) distances (2.011(9) and 2.036(8) Å) fall in the expected range,[7,22] the bond with the terminal C1 atom is slightly shorter, as expected. The C–C double bond length of 1.36(1) Å coincides with the value found in the complex [Cu(bipy)(styrene)]-(ClO_4)[22] and is slightly but significantly longer than the value commonly reported for free olefins (1.34 Å). The small lengthening of the C–C double bond confirms the presence of a slight but appreciable contribution from π-back-donation to the Cu^{I}–olefin bond.[18e,23]

It is interesting to compare the present structure with that of the trigonal bipyramidal platinum complex in which the same diamine is bound to the fragment [PtClMe((*E*)-ClCH=CHCl)].[13] Apart from the absence of axial substituents, one major difference is that in the present case both of the mesityl rings extend towards the coordinated olefin in an approximate C_2 symmetry, while in the platinum case this conformation is adopted only on one side of the molecule. A second relevant difference is that the chiral pocket created around the coordinated olefin is narrower and ≈0.5 Å deeper[24] in the copper complex than in the platinum complex as a result of the smaller size of the copper ion and the absence of axial ligands. These geometric differences can explain the essentially complete enantioface selectivity of the diamine–Cu^{+} fragment (in the C_2-symmetric configuration) versus the good but incomplete selectivity (84% in the propene case) observed for the platinum complex. Also, they can contribute to the much larger equilibrium constant for *R*/*S* exchange of the allylic alcohol, 1-butene-3-ol, in the copper complex (K ≈ 40) versus the platinum complex (K ≈ 4).

QM/MM modeling and chiral recognition: As shown above, the optimized geometries of complexes **3** (Figure 2) give a nice qualitative explanation of the exceptionally low δ values of some protons of the olefinic ligand (the same holds for the ethylene complexes **2**). Also, a fair semiquantitative agreement is found between the experimental result of only one enantioface being coordinated (within the detection limits) in the propene complex having the *R*, *S*, *S*, *R* arrangement of the diamine backbone (**3a**), and the relative energies of its most stable geometries (Table 4). Indeed, both the most stable structure **3a** (entries A1 and A3 in Table 4) and those structures higher in energy (3 kJ mol^{-1}) represented by entries B1, B3, C1 and C3 in Table 4 correspond to *re* propene coordination. In contrast, for *si* propene coordination, the most stable structure (entries B2 and C4 in Table 4) is 5 kJ mol^{-1} above that of **3a**. The lack of enantioface selectivity in the propene coordination to the asymmetric (*R*, *S*, *S*, *S*) diamine-Cu^{+} fragment, manifested in the comparable

Table 4. Relative steric energies [kJ mol^{-1}] of the QM/MM-optimized basic geometries of the propene complexes **3**.[a]

Entry		1 *re*	2 *si*	3 *re*	4 *si*
		Cu	Cu	Cu	Cu
A	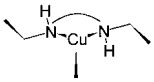	0(0) **3a**	9(15)	= A1	= A2
B	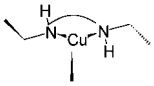	3(4)	5(5)	3(4)	(17)
C	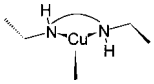	= B3	= B4	= B1	= B2
D	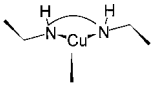	2(1) **3b**	2(1) **3c**	(11)	(16)
E	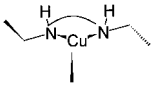	(20)	(21)	(22)	(34)
F	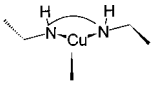	5(3)	5(3)	(13)	6(5)

[a] Values in parentheses come from pure MM calculations (see computional details).

populations of the two species **3b** and **3c** (Table 1), is also correctly predicted by the nearly equal energies (2 kJ mol^{-1}) of the corresponding optimized geometries (entries D1 and D2 in Table 4). However, the latter value is in significant disagreement with the experimentally found enthalpy difference (ca. 7 kJ mol^{-1}) between **3b** and **3a**. This might be explained by noting that in the optimized geometries for **3b** and **3c** (Figure 2) the approach of solvent or counterion to the Cu^{+} ion is possible only from the side of the N–H bonds, since approach from the other side is hindered by the two mesityl groups. The reduced stabilizing interactions between the metal ion and solvent or counterion in **3b** and **3c** relative to **3a** (not considered in the present QM/MM calculations) could account for the disagreement between the theoretical and experimental energy values and for a positive contribution to the entropy of **3b** and **3c** as actually found experimentally.[25] Further consistency is given to the above picture by the observation mentioned above that the asymmetric species **2b** (as well as **3b** and **3c**) undergoes olefin exchange at a much lower rate than **2a** and **3a**, most likely as a consequence of hindrance to a bimolecular substitution pathway.

0947-6539/00/0607-1134 $ 17.50+.50/0 *Chem. Eur. J.* **2000**, *6*, No. 7

The reason for the enantioface selection is easily seen from Figure 3A, where a front view of the lowest energy geometry of complex **3a** is displayed, showing, when the *re* face is coordinated, how the propene molecule fits into the chiral pocket created by the diamine ligand. The diamine-Cu^+ fragment keeps a virtually undistorted C_2 symmetry, indicating that no steric interaction exists between the propene methyl group and the adjacent mesityl ring, as confirmed by the essentially equal energies (3 kJ mol^{-1}) of the two conformations represented by entries B1 and B3 in Table 4. If the opposite enantioface is coordinated (Figure 3C), the diamine "arm" on the side of the propene methyl group is forced to twist back (entry B2 in Table 4) in order to avoid a strong steric interaction with the methyl group (Figure 3B, entries A2 and A4 in Table 4). The latter repulsive interactions force the olefin to rotate more than 30° out of the coordination plane, thus relieving the steric strain at the expense of reduction of electronic π-back-donation.

In the case of secondary allylic alcohols (and ethers), the reason for the large selectivity with regard to the coordination of the *R* enantiomer is suggested by the X-ray structure analysis of complex **8a** and nicely confirmed by the QM/MM analysis of complex **8**. In Figure 5, the crystal structure and the QM/MM optimized geometries of **8a** and **8c′** are compared. In the X-ray and calculated structures of **8a** (Figure 5A and 5B) the conformation of the diamine ligand looks similar to that calculated for the propene complex **3a** (Figure 3A), and that of the olefin ligand is such that the oxygen atom is pointing above the coordination plane, approaching the Cu^+ ion. In the QM/MM structure the distance between the oxygen atom and the metal is much shorter than that found in the crystal (2.73 Å versus 3.37 Å), as a consequence of the presence of the ClO_4^- counterion in the real structure. In fact, a QM/MM optimization of **8a**, in which a pure QM ClO_4^- counterion was included, gave a value for the Cu–OH distance equal to 3.42 Å, in good agreement with the experimental value. In the X-ray structure (as well as in the QM/MM structure including the counterion) a weak hydrogen bond between the OH group and the perchlorate anion is present.[26] An attractive interaction between the O atom and the Cu^+ ion was found in all the QM/MM low-energy geometries, including that of the very minor diastereomer **8c′** (Figure 5C). Thus, the orientation of the allylic oxygen atom towards the metal ion appears to be an attractive constraint acting on the complex. In the presence of this constraint, the coordination of the *R* enantiomer is forced by the need to have the *si* face coordinated[20] and to avoid steric contact between the olefinic methyl group and the nearby mesityl ring. Indeed, in the case of coordination of the *S* enantiomer, the QM/MM analysis indicates that in the preferred geometry the diamine backbone adopts the asymmetric *R*, *S*, *S*, *S* configuration and the opposite diastereoface is coordinated (Figure 5C).[27]

Implications on enantioselective catalysis: A major implication of our results is that the coordinated diamine (*S*,*S*)-**1** has a strong tendency to adopt a C_2-symmetric geometry as shown in Figures 2 (top) , 3A, 5A, and 5B. This geometry appears to be the most stable, unless the third ligand brings steric hindrance in two adjacent quadrants of the chiral space,[1] as in the case of *Z*-2-butene shown before. In the cases considered in this paper the third ligand is an olefin, but in a more general case it could be any other species, and the same steric requirements would control the geometry of the diamine. As mentioned in the introduction, (*S*,*S*)-**1** was successfully used in the catalytic enantioselective cyclopropanation of styrenes.[12] The suggested mechanism for this reaction assumes as the reactive species a copper(I) carbenoid intermediate, which should have the structure shown in Figure 6,[28] where the

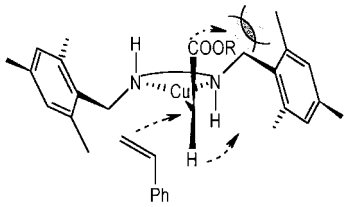

Figure 6. Schematic view of a disfavored styrene approach to a [Cu((*S*,*S*)-**1**)]-carbene intermediate in a catalyzed cyclopropanation reaction.

diamine adopts its preferred conformation. It is seen from Figure 6 that in the assumed mechanism,[28] the approach of a styrene molecule from the left side would push the ester group against the top of the mesityl ring on the right side in the transition state. This repulsive interaction would be reduced in the case of approach from the right side, leading to preferential reaction of the *re* enantioface in the case of *anti* orientation of the substituents (the *si* face in the case of the *syn* orientation). This is in agreement with the absolute configuration of the products (*trans*-**11** and *cis*-**11**) reported by Kanemasa et al.[12]

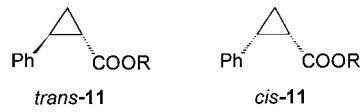

Conclusion

Throughout this work, a remarkable and consistent agreement between experimental and computational findings has been obtained. The overall results show that the diamine (*S*,*S*)-**1** creates a rather narrow and deep chiral pocket around the metal ion, enabling an efficient enantioface discrimination for olefins which are coordinated "in-plane" in a trigonal-planar arrangement. The (usually predominant) C_2-symmetric fragment, in which the two chiral nitrogen atoms display *R, R* configurations, shows an essentially complete selectivity for the coordination of the olefinic enantioface, filling the "empty" quadrants of the chiral space[1] (*re* face for propene and *E*-2-butene, *si* face for α-olefins other than propene).[20] The same fragment is capable of recognizing the *R* enantiomer of a secondary allylic alcohol or ether, displaying a large binding selectivity relative to the *S* enantiomer. The recognition is the combined result of the face selection and of the allylic oxygen atom being "hooked" on the side of the metal ion, so that only the enantiomer whose side chain points away

from the metal can fit in the chiral pocket. The asymmetric fragment, in which the two nitrogen atoms display *R, S* (or *S, R*) configurations, shows a poor enantioface selectivity in the case of α-olefins. This can be interpreted as the result of having both "empty" quadrants of the chiral space on the same side of the coordination plane. The actual abundance of the asymmetric fragment is strongly affected by other hindrance that might be present on the side of the coordination plane, which is going to be occupied by the *S*-nitrogen substituent. The asymmetric fragment is virtually absent in trigonal-bipyramidal Pt^{II} complexes,[13] (in which both sides are occupied by axial ligands) and in the *E*-2-butene complex **5** (in which both sides are hindered by the butene methyl groups). Conversely, the *R, S* configuration of the nitrogen atoms is relevant for the ethylene complex **2**, where no hindrance is present on either side of the coordination plane. It is even dominant for the *Z*-2-butene complex **6**, in which only one side of the coordination plane is free of hindrance but, at the same time, the C_2-symmetric diamine conformation would be much destabilized (as in Figure 3B for the propene molecule). Thus, a strong interplay takes place between the steric requirements carried by the olefin ligand and the configuration adopted by the diamine backbone.

As a final remark, we would like to point out that the consistent picture emerging from the present study has the potential to produce qualitative predictions concerning not only metal–olefin complexes of (*S,S*)-**1** but also other trigonally coordinate species of this important chiral auxiliary, which might be intermediates of enantioselective processes.

Experimental Section

General: NMR spectra were recorded on a 400 MHz Bruker model WH-400 spectrometer. CD_2Cl_2 and CD_3OD were used as solvents, and $CHDCl_2$ ($\delta = 5.31$) or $^{13}CD_2Cl_2$ ($\delta = 53.8$) as internal standards. The solvents were deaerated before use. All reactions were carried out under an argon atmosphere, with Schlenk techniques. The diamine **1**,[10] 3-methoxy-1-butene,[29] and the complex $[Cu(MeCN)_4]ClO_4$[30] were prepared according to previously described procedures.

Synthesis of [Cu((*S,S*)-1)(CH_2=CH_2)]ClO_4 (2): To a solution of $[Cu(MeCN)_4]ClO_4$ (0.080 g, 0.24 mmol) in CH_2Cl_2 (3 mL) solid (*S,S*)-**1** (0.116 g, 0.24 mmol) was added. At 233 K, ethylene was bubbled through the solution until a white solid precipitated. The solid was dissolved by warming the mixture to room temperature, then white crystals were obtained by cooling again to 243 K. The solvent was removed by filtration and the crystals were washed with pentane and dried. Yield of **2**: 0.120 g (75%). ^{13}C NMR (CD_2Cl_2/CD_3OD 450 μL/40 μL, 263 K): (**2a**) $\delta = 19.6$ (*o-Me*Ph), 20.6 (*p-Me*Ph), 46.5 (NCH_2), 69.3 (*C*HPh), 80.2 (CH_2=); (**2b**) $\delta = 19.6$ (*o-Me*Ph), 20.6 (*p-Me*Ph), 41.2 (NCH_2), 47.0 ($NC'H_2$), 64.5 (*C*HPh), 64.6 (*C'*HPh), 80.9 (CH_2=); $C_{36}H_{44}ClCuN_2O_4$ (667.7) (%): calcd: C 64.75, H 6.64, N 4.20; found: C 64.42, H 6.70, N 4.22.

Synthesis of [Cu((*S,S*)-1)(CH_2=CHMe)]ClO_4 (3): The same procedure was followed as for **2**, without recrystallizing the product. ^{13}C NMR (CD_2Cl_2/CD_3OD 450 μL/40 μL, 253 K): $\delta = 18.1$ (=CH*Me*), 19.7 (*o-Me*Ph), 20.6 (*p-Me*Ph), 46.5 (NCH_2), 69.0 (*C*HPh), 80.6 (CH_2=), 98.5 (=*C*HMe); $C_{37}H_{46}ClCuN_2O_4$ (681.8) (%): calcd: C 65.18, H 6.80, N 4.11; found: C 65.02, H 6.93, N 4.20.

Synthesis of [Cu((*S,S*)-1)(*E*-MeCH=CHMe)]ClO_4 (5) and [Cu((*S,S*)-1)(*Z*-MeCH=CHMe)]ClO_4 (6): The same procedure was followed as for **3**. **5:** ^{13}C NMR (CD_2Cl_2/CD_3OD 450 μL/40 μL, 233 K): $\delta = 17.3$ (=CH*Me*), 18.7 (*o-Me*Ph), 20.7 (*p-Me*Ph), 21.2 (*o-Me*Ph), 47.0 (NCH_2), 68.9 (*C*HPh), 96.4 (CH=); $C_{38}H_{48}ClCuN_2O_4$ (695.8)(%): calcd: C 65.60, H 6.95, N 4.03; found: C 65.43, H 6.83, N 4.15. **6:** $C_{38}H_{48}ClCuN_2O_4$ (695.8) (%): calcd: C 65.60, H 6.95, N 4.03; found: C 65.48, H 6.87, N 4.13.

Synthesis of [Cu((*S,S*)-1)(CH_2=CHR)]ClO_4 (R = C_3H_7 (4); R = CH_2OH (7); R = CH(OH)C_5H_{11}, (9); R = CH(OMe)Me (10)): To a solution of $[Cu(MeCN)_4]ClO_4$ (0.080 g, 0.24 mmol) in CH_2Cl_2 (3 mL, for **9** only 1.5 mL), solid (*S,S*)-**1** (0.116 g, 0.24 mmol) was added. At room temperature the appropriate olefin (1.20 mmol) was added. After 24 h at 253 K, white crystals were formed. The solvent was removed by filtration and the crystals were washed with pentane and dried. Yield: 80–90%. **4**: $C_{39}H_{50}ClCuN_2O_4$ (709.8) (%): calcd: C 65.99, H 7.10, N 3.95; found: C 65.98, H 7.14, N 3.94. **7**: $C_{37}H_{46}ClCuN_2O_5$ (697.8) (%): calcd: C 63.69, H 6.64, N 4.01; found: C 63.45, H 6.54, N 4.14. **9**: ^{13}C NMR (CD_2Cl_2/CD_3OD 450 μL/40 μL, 253 K): $\delta = 14.0$ ($(CH_2)_4$*Me*), 20.0 (*o-Me*Ph), 20.6 (*p-Me*Ph), 47.3 (NCH_2), 69.7 (*C*HPh), 70.6 (CHOH), 72.4 (CH_2=), 109.5 (=CH); $C_{42}H_{56}ClCuN_2O_5$ (767.9) (%): calcd: C 65.69, H 7.35, N 3.65; found: C 65.43, H 7.19, N 3.76. (10) ^{13}C NMR (CD_2Cl_2/CD_3OD 450 μL/40 μL, 253 K): $\delta =$ 20.1 (*o-Me*Ph), 20.3 (CH(OMe)*Me*), 21.0 (*p-Me*Ph), 47.7 (NCH_2), 55.8 (OCH_3), 70.2 (*C*HPh), 74.0 (*C*HOMe), 75.1 (CH_2=), 103.3 (=CH); $C_{39}H_{50}ClCuN_2O_5$ (725.8) (%): calcd: C 64.54, H 6.94, N 3.86; found: C 64.33, H 6.82, N 3.94.

Synthesis of [Cu((*S,S*)-1)((*R*)-CH_2=CHCH(OH)Me)]ClO_4 (8a): To a solution of $[Cu(MeCN)_4]ClO_4$ (0.080 g, 0.24 mmol) in acetone (5 mL), solid (*S,S*)-**1** (0.116 g, 0.24 mmol) was added. At room temperature, racemic 1-buten-3-ol (104 μL, 1.20 mmol) was added. After 24 h at 253 K, white crystals were formed. The solvent was removed by filtration and the crystals were washed with pentane and dried. Yield of **8a** · C_3H_6O: 0.175 g (95%). To obtain crystals suitable for X-ray diffraction analysis, the same procedure as above was used, in a more dilute acetone solution (20 mL). No recrystallization was performed. ^{13}C NMR (CD_2Cl_2/CD_3OD 450 μL/40 μL, 253 K): $\delta = 19.5$ (*o-Me*Ph), 20.5 (*p-Me*Ph), 23.9 (CH(OH)*Me*), 47.2 (NCH_2), 66.2 (CHOH), 69.6 (CHPh), 71.5 (CH_2=), 105.5 (=CH); $C_{38}H_{48}ClCuN_2O_5 \cdot C_3H_6O$ (769.9) (%): calcd: C 63.96, H 7.07, N 3.64; found: C 64.00, H 7.02, N 3.69.

Resolution of 1-buten-3-ol: Complex **8a** (2.18 g, 1.7 mmol) was suspended in a 2.5 M HCl solution (10 mL), and diethyl ether (10 mL) was added under stirring. The mixture was stirred for 20 min at room temperature, centrifuged, and the diethyl ether layer was collected. After two further extractions with diethyl ether (10 mL), the organic phase was dried over Na_2SO_4. The solvent was removed and a fractional distillation gave (*R*)-1-buten-3-ol (0.106 g) in 93% *ee*.

X-ray crystallography: The details of the structure analysis are listed in Table 5. X-ray data were collected on an Enraf-Nonius CAD4-F diffractometer using $Cu_{K\alpha}$ graphite-monochromated radiation operated in the ω/θ scan mode. The unit cell parameters were obtained by a least-squares

Table 5. Crystal data and structure refinement parameters for **8a**.

crystal size [mm]	$0.20 \times 0.20 \times 0.60$
formula	$C_{38}H_{48}ClCuN_2O_5 \cdot C_3H_6O$
formula weight	769.9
crystal system	orthorhombic
space group	$P2_12_12_1$
a [Å]	12.380(3)
b [Å]	15.080(5)
c [Å]	21.868(7)
V [Å^3]	4083(2)
Z	4
$F(000)$	1632
ρ_{calcd} [g cm^{-3}]	1.253
$\rho_{measured}$ [g cm^{-3}]	1.24
$\lambda(Cu_{K\alpha})$ [Å]	1.54056
θ_{max} [°]	75
μ [cm^{-1}]	17.1
no. independent reflections	4611
no. reflections above $3\sigma(I)$	3322
no. refined parameters	440
goodness of fit	1.185
R	0.063
wR	0.075

0947-6539/00/0607-1136 $ 17.50+.50/0 *Chem. Eur. J.* **2000**, *6*, No. 7

fitting of the setting values of 25 strong reflections in the range $25^\circ < \theta < 28^\circ$. Three monitoring reflections, measured every 400 reflections, showed only tiny intensity fluctuations. The structure was solved by routine application of the Patterson and Fourier techniques. A molecule of acetone was detected in a difference electron density map. The full-matrix least-squares refinement minimized the quantity $\Sigma w(\Delta F)^2$ with $w^{-1} = [\sigma^2(F_o) + (0.02\,F_o)^2 + 1]$ where σ is derived from counting statistics. All non-hydrogen atoms were refined anisotropically except those of the solvent molecule. The hydrogen atoms, added on the basis of geometric considerations and difference Fourier suggestions, were assigned the isotropically equivalent thermal parameters of the carrier atoms and included in the final refinement as riding atoms. A correction for absorption effects was applied according to Walker and Stuart[31] by using the DIFABS computer program (maximum and minimum values of the absorption correction were 1.6 and 0.8). The absolute value of the highest positive or negative peaks in the final difference Fourier map was not larger than 0.5 e Å^{-3}.

All calculations were performed with the Enraf-Nonius (SDP) set of programs.[32] Crystallographic data (excluding structure factors) for the structure reported in this paper have been deposited with the Cambridge Crystallographic Data Centre as supplementary publication no. CCDC-132619. Copies of the data can be obtained free of charge on application to CCDC, 12 Union Road, Cambridge CB2 1EZ, UK (fax: (+44) 1223 336–033; e-mail: deposit@ccdc.cam.ac.uk).

Computational details: To locate the minimum energy geometries, the following procedure was followed. For the ethylene complex with the *R*, *S*, *S*, *R* configuration of the diamine ligand, we performed a systematic search by varying the torsional angles around the N–C(mesityl) bonds, while optimizing all other degrees of freedom. This procedure allowed us to select six independent conformations of the ethylene complex with energy below the threshold of 40 kJ mol^{-1} relative to the absolute energy minimum. After this search, energy optimizations on propene complexes with the ligand presenting all the minimum energy conformations selected above, were performed. Coordination of both propene enantiofaces and different propene orientations were considered. A similar approach was also used to locate the minimum energy geometries for complexes containing the chiral alcohol. Since these systematic calculations involve a large number of conformations, they are beyond feasibility with current computational resources even with the relatively fast QM/MM approach. Hence, they were performed with the computationally cheap MM approach. For all of the complexes considered, geometries which presented MM energies below the threshold of 10 kJ mol^{-1} relative to the absolute MM energy minimum were refined with the more reliable QM/MM method. The validity of this approach is confirmed by the substantial agreement between the relative stability of different geometries obtained with the MM and QM/MM methods. To demonstrate the relatively good agreement between the MM and QM/MM results for the case of the propene complexes, both the MM and QM/MM energies are reported in Table 4. A similar approach was used to locate the minimum energy geometries for the complexes with the *R*, *S*, *S*, *S* configuration of the diamine ligand.

Pure molecular mechanics (MM) calculations: The results presented in this paper were obtained with the CHARMM force field of Karplus et. al.[33] To model the olefin coordination to the metal atom, the dummy atom approach, extensively used to simulate the coordination of π ligands (olefins, aromatic rings) to transition metals, has been adopted.[23,34,35] Since the CHARMM force field has not been extended to copper complexes, we had to make some assumptions about the force field parameters needed to simulate both diamine and olefin coordination to the copper atom. The Cu–N and Cu–D equilibrium distances, where "D" is the dummy atom located in the center of the olefin double bond, have been assumed to be 2.05 and 1.93 Å, respectively. Moreover, the N-Cu-N and N-Cu-D equilibrium angles have been assumed to be 90° and 135°, respectively. These values approximately correspond to those observed in the X-ray structure of compound **8**. As for the associated bond stretching and angle bending force constants, they have been assumed to be equal to the Zr–D_{Cp} and D_{Cp}-Zr-D_{Cp} force constants proposed by Bosnich et. al. in their extension of the CHARMM force field to include Group 4 metallocenes.[34] The remaining parameters needed to simulate olefin coordination to the copper atom have been assumed to be equal to the analogous parameter proposed by Bosnich et. al. to simulate the coordination of the cyclopentadienyl ring to Group 4 metals.[34] In all of the MM calculations, the Cu and N atoms, and the center of the olefin double bond have been forced to lie in the same plane. No potential has been used to control the rotation of the olefin out of the N-Cu-N plane. However, these rotations were constrained to be smaller than 10°. All the van der Waals parameters have been derived from the CHARMM force field.[33] Copper was assigned the "Cu3 + 1" van der Waals parameters of Rappé's UFF.[36] To prevent the effect of long-range attractive forces,[37,38,39] for van der Waals interactions we have assumed pure repulsive potentials as described in detail in references [38,39]. Electrostatic interactions were not included in the molecular mechanics potential. This approach has been extensively used to rationalize a large number of experimental facts in the field of propene polymerization with both heterogeneous[40] and homogeneous catalysts,[38,41] the mechanism of enantioselectivity in both primary and secondary propene insertion, in particular.

Combined quantum mechanics and molecular mechanics (QM/MM) calculations: The QM/MM calculations were performed with the ADF density functional theory program,[42,43] modified by some of us[44,45] to include standard molecular mechanics force fields in such a way that the QM and MM parts are coupled self-consistently, according to the method prescribed by Morokuma and Maseras.[46] The model QM system and the real QM/MM systems are reported in Scheme 2. The partitioning of the

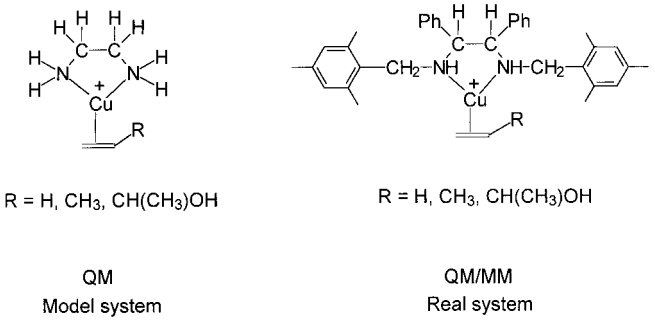

Scheme 2.

systems into QM and MM parts only involves the substituents on the diamine ligand, that is, the five-membered diamine ligand including the metal atom. The considered olefins (ethylene, propene, 1-buten-3-ol), are always totally composed by pure QM atoms. The only MM atoms are hence the CH_2-mesityl and phenyl substituents on the diamine ligand. The connection between the QM and MM parts occurs by means of the so-called capping "dummy" hydrogen atoms, which are present in the model system only.[46] These capping atoms are replaced in the real system by the corresponding "linking" carbon atom.[46] For example, the trasformation of one of the C–H bonds of the ligand into the C–Ph group involves the replacement of the H atom in the model QM system with a C atom in the real QM/MM system. The QM and MM parts are thus linked by the "capping" hydrogen atoms and coupled by van der Waals interactions. The geometric optimization on the whole system was carried out within this coupling scheme between QM and MM atoms. In the optimization of the MM part, the N–C and C–C bonds crossing the QM/MM border were constrained to be 0.45 and 0.40 Å longer than the corresponding optimized N–H and C–H distances, providing optimized N–C and C–C distances in the real system of roughly 1.50 and 1.52 Å, respectively. Further details on the methodology can be found in previous papers.[44,45,46]

As for the DFT calculations on the cationic QM part, the electronic configuration of the molecular systems were described by a triple-ξ STO basis set on copper for 3s, 3p, 3d, 4s, and 4p. Double-ξ STO basis sets were used for nitrogen and carbon 2s and 2p, and hydrogen 1s, augmented with a single 3d and 2p function, respectively.[47,48] The inner shells on copper (up to 2p) and nitrogen and carbon (1s), were treated within the frozen core approximation. Energies and geometries were evaluated with the local exchange-correlation potential by Vosko et. al.,[49] augmented in a self-consistent manner with Becke's[50] exchange gradient correction and Perdew's[5152] correlation gradient correction.

As for the molecular mechanics potential, the CHARMM force field developed by Karplus et. al.[33] has been adopted. The only MM parameter needed for copper is the van der Waals potential (Cu3 + 1 taken from the

Rappé's UFF),[36] since coordination of the diamine ligand and the olefin to the metal are treated within the QM part. In the pure MM calculations, a repulsive function has been used for the van der Waals interactions, and no electrostatic interactions were included in the MM potential.

All of the calculated structures represent energy minima on the combined QM/MM potential surface. Geometric optimizations were terminated if the largest component of the Cartesian gradient was smaller than 0.002 au. This combined QM/MM approach has previously been utilized to study the enthalpy of ligand substitution on Ru and Fe complexes,[39] the ethylene polymerization with homogeneous catalysts based on early transition metals[53] as well as on late transition metals,[45] and to make predictions on the *E*/*Z* selectivity in ethylene/2-butene copolymerization with Group 4 metallocenes.[54]

Acknowledgements

The authors thank the MURST project: "New strategies for the control of reactions: interaction of molecular fragments with metallic sites in non-conventional species" for financial support and the CIMCF, Università di Napoli "Federico II" for access to NMR and X-ray facilities.

[1] J. A. Gladysz, B. J. Boone, *Angew. Chem.* **1997**, *109*, 566; *Angew. Chem. Int. Ed. Engl.* **1997**, *36*, 550.
[2] a) *Advances in Catalytic Processes*, *Vol. 1* (Ed.: M. P. Doyle), Jai Press Inc., London, **1995**; b) *Advances in Catalytic Processes*, *Vol. 2* (Ed.: M. P. Doyle), Jai Press Inc., London, **1997**.
[3] A paradigmatic case is the homogeneous rhodium-catalyzed asymmetric hydrogenation. See J. M. Brown, *Chem. Soc. Rev.* **1993**, 25.
[4] For example trigonal copper(I) olefin complexes such as those described in this paper might serve as steric models of the palladium(0) intermediates following the transition state of asymmetric allylic alkylation. See: a) S. Ramdeehul, P. Dierkes, R. Aquado, P. C. Kamer, P. W. N. M. van Leeuwen, J. A. Osborn, *Angew. Chem.* **1998**, *110*, 3302; *Angew. Chem. Int. Ed.* **1998**, *37*, 3118; b) E. Peña-Cabrera, P.-O. Norrby, M. Sjögren, A. Vitagliano, V. De Felice, J. Oslob, S. Ishii, D. O'Neill, B. Åkermark, P. Elquist, *J. Am. Chem. Soc.* **1996**, *118*, 4299.
[5] a) M. E. Cucciolito, F. Ruffo, A. Vitagliano, M. Funicello, *Tetrahedron Lett.* **1994**, *35*, 169; b) G. Paiaro, *Organomet. Chem. Rev. A* **1970**, *6*, 319, and references therein.
[6] a) M. S. Visser, N. M. Heron, M. T. Didiuk, J. F. Sagal, A. H. Hoveyda, *J. Am. Chem. Soc.* **1996**, *118*, 4291; b) M. S. Visser, J. P. A. Harrity, A. H. Hoveyda, *J. Am. Chem. Soc.* **1996**, *118*, 3779; J. P. Morken, M. T. Didiuk, M. S. Visser, A. H. Hoveyda, *J. Am. Chem. Soc.* **1994**, *116*, 3123; M. Kitamura, I. Kasahara, K. Manabe, R. Noyori, H. Takaya, *J. Org. Chem.* **1988**, *53*, 708.
[7] R. W. Quan, Z. Li, E. N. Jacobsen, *J. Am. Chem. Soc.* **1996**, *118*, 8156.
[8] See for example: a) A. Carmona, A. Corma, M. Iglesias, F. Sánchez, *Inorg. Chim. Acta* **1996**, *244*, 239; b) P. J. Pérez, M. Brookhart, J. L. Templeton, *Organometallics* **1993**, *12*, 261; c) Z. Li, R. W. Quan, E. N. Jacobsen, *J. Am. Chem. Soc.* **1995**, *117*, 5889.
[9] a) M. van Klaveren, E. S. M. Persson, A. del Villar, D. M. Grove, J.-E. Bäckvall, G. van Koten, *Tetrahedron Lett.* **1995**, *36*, 3059; b) E. S. M. Persson, M. van Klaveren, D. M. Grove, J.-E. Bäckvall, G. van Koten, *Chem. Eur. J.* **1995**, *1*, 351.
[10] E. J. Corey, P. DaSilva Jardine, S. Virgil, P. W. Yuen, R. D. Connell, *J. Am. Chem. Soc.* **1989**, *111*, 9243.
[11] a) Y. Wang, S. A. Babirad, Y. Kishi, *J. Org. Chem.* **1992**, *57*, 468; b) J. U. Jeong, P. L. Fuchs, *J. Am. Chem. Soc.* **1994**, *116*, 773.
[12] S. Kanemasa, S. Hamura, E. Harada, H. Yamamoto, *Tetrahedron Lett.* **1994**, *35*, 7985.
[13] M. E. Cucciolito, M. A. Jama, F. Giordano, A. Vitagliano, V. De Felice, *Organometallics* **1995**, *14*, 1152.
[14] The diamine **1** was always used in almost enantiomerically pure form. It was prepared and resolved by us and both (*S*,*S*)-**1** and (*R*,*R*)-**1** enantiomers were available. Most experiments were performed using (*S*,*S*)-**1** but in some cases the *R, R* enantiomer was used. To avoid confusion in presenting the results, throughout this paper we consistently refer to the use of (*S*,*S*)-**1**.
[15] Although allowed by symmetry, the alternate possibility, *S*, *S*, *S*, *S*, is too unlikely on steric grounds to be considered as the configuration of a major species.
[16] Y. D. Wu, Y. Wang, K. N. Houk, *J. Org. Chem.* **1992**, *57*, 1362.
[17] F. P. Intini, L. Maresca, G. Natile, A. Pasqualone, *Inorg. Chim. Acta* **1994**, *227*, 261.
[18] a) J. S. Thompson, R. L. Harlow, J. F. Whitney, *J. Am. Chem. Soc.* **1983**, *105*, 3522; b) J. S. Thompson, R. M. Swiatek, *Inorg. Chem.* **1985**, *24*, 110; c) J. S. Thompson, J. F. Whitney, *Inorg. Chem.* **1984**, *23*, 2813; d) H. Masuda, N. Yamamoto, T. Taga, K. Machida, S. Kitagawa, M. Munakata, *J. Organomet. Chem.* **1987**, *322*, 121; e) M. Munakata, S. Kitagawa, S. Kosome, A. Asahara, *Inorg. Chem.* **1986**, *25*, 2622.
[19] We tried to get independent evidence of the mutual spatial arrangements of the olefin and the mesityl rings through NOE measurements. However, no NOE effect was detected, probably because trace amounts of the paramagnetic Cu^{2+} ion were present.
[20] Confusion should be avoided by keeping in mind that according to the *re-si* nomenclature convention, a formal inversion takes place in going from propene to any higher α-olefin. That is, the same enantioface that is named *re* in the propene molecule, is named *si* in the case of higher olefins and vice-versa.
[21] Y. Ishino, T. Ogura, K. Noda, T. Hirashima, O. Manabe, *Bull. Chem. Soc. Japan* **1972**, *45*, 150.
[22] H. Masuda, K. Machida, M. Munakata, S. Kitagawa, H. Shimono, *J. Chem. Soc. Dalton Trans.* **1988**, 1907, and references therein.
[23] F. Hæffner, T. Brinck, M. Haeberlein, C. Moberg, *Theochem.* **1997**, *397*, 39.
[24] A geometric analysis of the depth of the chiral pocket can be performed by setting the plane defined by the metal and the two olefinic carbons as the *xy* plane, the *x* axis oriented along the C–C double bond, the metal atom in the negative *y* direction, and looking at the *y* coordinate of the *p*-carbon of the mesityl ring(s). In the copper complex the *y* coordinate of C33 is about 0.0 Å and that of C12 is +0.3 Å, while in the platinum complex the *y* coordinate of the corresponding atom (C9 in the cited structure)[12] is −0.5 Å. Also, in the copper complex the distance between the olefinic carbon(s) and the middle point of the nearby mesityl ring are 3.7 Å and 3.8 Å for C1 and C2, respectively, while in the platinum complex the corresponding distance is 4.2 Å.
[25] A further decrease in stability of the asymmetric *R*, *S*, *S*, *S* configuration is observed in the case of allylic alcohols and ethers (see Table 1) and can also be rationalized. Since in this arrangement the copper ion is hindered on one side of the coordination plane, the interactions with the counterion or solvent on the "open" side should be stronger, thus leaving less room for the intramolecular interaction with the alcoholic oxygen and reducing the overall relative stability compared with the symmetric configuration *R*, *S*, *S*, *R*.
[26] Hydrogen bonding between the OH group and the counterion (possibly occurring in close-tight ion pairs) is not relevant for the chiral recognition of the *R* enantiomer, since substitution of a methoxy group for the oxydryl in the 3-methoxy-1-butene complex **10** did not affect the selectivity.
[27] The QM/MM analysis calculates **8c′** to be only 1 kJ mol^{-1} above **8a**. This is in quantitative disagreement with the experiment but can be explained in the same way as the propene case (see also reference [25]).
[28] See reference [2a], p. 69.
[29] J. B. Baruah, A. G. Samuelson, *J. Chem. Soc. Chem. Commun.* **1987**, 36.
[30] P. Hemmerich, C. Sigwart, *Experientia* **1963**, *15*, 488.
[31] N. Walker, D. Stuart, *Acta Crystallogr. Sect. A* **1983**, *39*, 158.
[32] B. A. Frenz & Associates Inc. Structure Determination Package (SDP), College Station, TX, and Enraf-Nonius, Delft, The Netherlands, **1982**.
[33] B. R. Brooks, R. E. Bruccoleri, B. D. Olafson, D. J. States, S. Swaminathan, M. Karplus, *J. Comput. Chem.* **1983**, *4*, 187.
[34] T. N. Doman, T. K. Hollis, B. Bosnich, *J. Am. Chem. Soc.* **1995**, *117*, 1352.
[35] U. Höweler, R. Mohr, M. Knickmeier, G. Erker, *Organometallics* **1994**, *13*, 2380.
[36] A. K. Rappé, C. J. Casewit, K. S. Colwell, W. A. Goddard III, W. M. Skiff, *J. Am. Chem. Soc.* **1992**, *114*, 10024.

  0947-6539/00/0607-1138 $ 17.50+.50/0 *Chem. Eur. J.* **2000**, *6*, No. 7

[37] R. R. Sauers, *J. Chem. Educ.* **1996**, *73*, 114.
[38] G. Guerra, P. Longo, L. Cavallo, P. Corradini, L. Resconi, *J. Am. Chem. Soc.* **1997**, *119*, 4394.
[39] L. Cavallo, T. K. Woo, T. Ziegler, *Can. J. Chem.* **1998**, *76*, 1457.
[40] P. Corradini, V. Barone, R. Fusco, G. Guerra, *Eur. Polym. J.* **1979**, *15*, 133.
[41] G. Guerra, L. Cavallo, G. Moscardi, M. Vacatello, P. Corradini, *J. Am. Chem. Soc.* **1994**, *116*, 2988.
[42] ADF 2.3.0, Vrije Universiteit Amsterdam: Amsterdam, The Netherlands, **1996**.
[43] E. J. Baerends, D. E. Ellis, P. Ros, *Chem. Phys.* **1973**, *2*, 41.
[44] T. K. Woo, L. Cavallo, T. Ziegler, *Theor. Chem. Acc.* **1998**, *100*, 307.
[45] L. Deng, T. K. Woo, L. Cavallo, P. M. Margl, T. Ziegler, *J. Am. Chem. Soc.* **1997**, *119*, 6177.
[46] F. Maseras, K. Morokuma, *J. Comput. Chem.* **1995**, *16*, 1170.
[47] J. G. Snijders, P. Vernooijs, E. J. Baerends, *At. Nucl. Data Tables* **1981**, *26*, 483.
[48] P. Vernooijs, J. G. Snijders, E. J. Baerends, *Slater Type Basis Functions for the whole Periodic System*; Vrije Universiteit Amsterdam: Amsterdam, The Netherlands, **1981**.
[49] S. H. Vosko, L. Wilk, M. Nusair, *Can. J. Phys.* **1980**, *58*, 1200.
[50] A. Becke, *Phys. Rev. A* **1988**, *38*, 3098.
[51] J. P. Perdew, *Phys. Rev. B* **1986**, *33*, 8822.
[52] J. P. Perdew, *Phys. Rev. B* **1986**, *34*, 7406.
[53] P. M. Margl, T. K. Woo, T. Ziegler, *Organometallics* **1998**, *17*, 4997.
[54] G. Guerra, P. Longo, P. Corradini, L. Cavallo, *J. Am. Chem. Soc.* **1999**, *121*, 8651.

Received: July 26, 1999 [F1934]